NASA Contractor Report 185260
AIAA-90-1990

Multi-sensor Analysis Techniques for SSME Safety Monitoring

William A. Maul III
Sverdrup Technology, Inc.
Lewis Research Center Group
Brook Park, Ohio

June 1990

Prepared for
Lewis Research Center
Under Contract NAS3-25266

National Aeronautics and
Space Administration

Multi-sensor Analysis Techniques for SSME Safety Monitoring

William A. Maul III
Sverdrup Technology, Inc.
Lewis Research Center Group
Brook Park, Ohio 44142

Abstract

Two algorithms were developed which utilized multi-sensor analysis techniques to complement the current Space Shuttle Main Engine (SSME) safety monitoring system. The first algorithm analyzed the accumulative error between actual and predicted values of the engine parameter set, while the second algorithm combined these error terms into a response pattern and correlated each pattern with a standard pattern. These algorithms were applied to twelve SSME anomalous test firings and were found to produce improved failure detection times in eight of those twelve compared to the current engine safety monitoring system. Of the eight detected anomalous test firings, the first algorithm detected all eight, while the second algorithm detected seven of the eight. No false alarms were indicated by either algorithm for twelve nominal test firings. An initial parametric study of these algorithms for optimized parameter selection is presented and algorithm robustness to sensor failure is demonstrated.

Nomenclature

ADD	Accumulative Difference Detection
ARMA	Autoregressive Moving Average
a	Linear Coefficients
Cov	Covariance Function
D(t)	Normalized Difference Value
E(t)	Engine Error Value
HMSRE	Health Management System for Rocket Engines
HPFP	High Pressure Fuel Pump
HPFT	High Pressure Fuel Turbine
HPFTP	High Pressure Fuel TurboPump
HPOT	High Pressure Oxidizer Turbine
LOX	Liquid Oxygen
LPFP	Low Pressure Fuel Pump
LPOP	Low Pressure Oxidizer Pump
MCC	Main Combustion Chamber
P	Predicted Value of Sensor
P(t)	Normalized Difference Pattern
PBM	Power Balance Model
PBP	Preburner Boost Pump
PID	Parameter Identification number
R(t)	Correlation Coefficient
RPL	Rated Power Level
S(t)	Actual Sensor Value
SAFD	System for Anomaly and Failure Detection
SD	Standard Deviation Function
SSME	Space Shuttle Main Engine
ZTO	Zero Template with Offset term

Introduction

An analytical investigation was conducted to develop new failure detection algorithms which provide additional capabilities to the current state of rocket engine safety monitoring. These new algorithms must have the ability to analyze the engine's data and detect anomalous engine behavior in real-time. They must also minimize the possibility of false alarms, while at the same time provide enough advance warning to enable the controller to halt engine operation and prevent further engine damage.

Current efforts in the advancement of safety monitoring technology are focused upon the Space Shuttle Main Engine (SSME), because it is an operational, reuseable rocket engine that has had testing failures resulting in major engine damage. The current SSME safety monitoring system applies a limited detection package to a small set of conventional sensors. This package analyzes

five parameters individually and indicates imminent engine failure based upon hardware limitations. Often when these limitations are exceeded, the ability to minimize the damage to the engine has been lost.

Over 1300 hot-fire test have been conducted for the SSME since 1976. Despite the current monitoring package, reference 1 reported forty tests resulted in damage, cost and time delay effects due to engine anomalies. Cikanek's investigations, references 2 and 3, classify twenty-seven of these forty anomalies as major incidents resulting in substantial hardware damage and loss. Also reported in reference 3, from 1976-1984 the current controller initiated over 200 engine cutoffs that were a result of false alarms. The purpose of this investigation was to develop failure detection algorithms which complement the current SSME safety monitoring system without indicating additional false alarms.

Recently, a number of investigations have been conducted to apply various detection algorithms to SSME test stand data. Some techniques analyze the response from single sensor outputs, while others utilize a collage of sensor data. Single sensor techniques allow for better detection of failure modes that manifest themselves in a few sensors. However, multi-sensor techniques are sensitive to failure modes that cause small deviations in a number of performance sensors.

Examples of applied single sensor techniques are the ARMA algorithm reported in reference 4 and, the SAFD algorithm reported in references 1 and 5. The Autoregressive Moving Average (ARMA) algorithm utilized time series analysis techniques, while the System for Anomaly and Failure Detection (SAFD) scheme utilized a two-second moving average of the data. Other approaches, references 4 and 6, combined sensor information in order to detect an anomalous engine response. In reference 4, researchers correlated engine response patterns, while researchers in reference 6, applied an accumulative error approach in the Health Management System for Rocket Engines (HMSRE) algorithm.

Rocket engine failure modes can be classified into two groups dependent upon the available preliminary indications to failure. One group has the characteristic that there is little or no indication prior to actual failure. It includes failures, such as duct rupture and some turbine blade failure modes. The other group has precursor information, distributed throughout the system and reflected by changes in system performance. For these failures, earlier detection would allow the controller to interrupt the failure mode and thus reduce further engine damage. The multi-sensor techniques are capable of detecting precursory information of this type, therefore their incorporation into a monitoring system would provide improved rocket engine safety.

The reported investigation was begun, following a review of the multi-sensor algorithms reported in recent SSME health management framework studies, references 4 and 6, conducted through NASA Lewis Research Center. The two algorithms developed for this report utilize the multi-sensor analysis techniques presented in those studies. This investigation expands upon those studies by addressing implementation issues of the techniques, such as sensor set optimization, sensor failure robustness and establishment of detection limits. The first algorithm analyzes the accumulative error between actual and predicted values of the engine sensor set, while the second algorithm combines these error terms into a response pattern and correlates each pattern with a standard pattern. The evaluation of these algorithms was based upon SSME test data; 12 nominal tests and 12 tests containing failure data.

Algorithm Development

Both algorithms developed in this investigation provided detection only during steady state engine operation. Every 40 milliseconds, each sensor in the data set was compared to a nominal standard value of that sensor for the given operating conditions. Twenty-four sensors were selected for analysis. These sensors are currently available to the SSME controller and are predicted by the Power Balance Model (PBM). The SSME PBM was used to calculate the nominal standard values for each sensor at various operating power levels. The other operating conditions, such as the fuel and oxidizer inlet conditions, were held constant for the PBM simulation, because as reported in reference 4, they have much less effect upon the sensors. Polynomial regression models were then developed for each sensor to provide a curve fitting of the PBM data as a function of commanded engine power level.

After analysis of the data, the low pressure oxidizer pump (LPOP) discharge pressure and the high pressure oxidizer turbine (HPOT) discharge temperature were eliminated from the sensor test sets due to their variations during the liquid oxygen (LOX) venting procedure. This procedure is regulated by human operators and its occurrence depends upon the test objectives. The regression models used in this investigation were unable to predict the effects due to LOX venting. The low pressure fuel pump (LPFP) discharge pressure parameter was also deleted from the test sets due to extreme unsteadiness of the values during constant power-level engine operation.

The eighteen remaining sensors were separated into fuel-side and LOX-side performance sensor sets as shown in Table 1. Each sensor set also contained the controller reference main combustion chamber (MCC) pressure which was used by the algorithms to determine the current operating conditions. The preburner boost pump (PBP) discharge pressure was included in both sets, because this sensor measured the oxidizer pressure supplied to both the fuel and oxidizer preburners. Each sensor set was analyzed by both algorithms, along with a total sensor set that contained all eighteen sensors.

Data Processing

Development of the algorithms involved normalizing SSME test sensor data to merge diverse engine information. This allowed diverse sensors that vary in magnitude and type of measured quantity, to be incorporated together in a single algorithm. In equation form, the processing of the data set appears as,

$$D(t)_i = 1 - \frac{S(t)_i}{P_i}, \tag{1}$$

where $D(t)_i$ is the normalized difference value, $S(t)_i$ is the actual sensor value at time t and P_i is the predicted value for sensor i. Using equation (1) eliminates the nominal predicted element from the sensor information, and the normalized real effect elements remain.

Accumulative Difference Detection Algorithm

The first algorithm evaluated involved detection based upon the magnitude of the normalized error values from equation (1). This algorithm was applied during constant power-level regions of the engine's test profile. The main feature of this algorithm is it's capability of detecting engine failure modes that manifest themselves as small magnitude changes in a number of performance parameters.

For an ideal case, the regression models would predict the system exactly and the normalized difference values would be zero throughout the test firing. From actual nominal test firings, the normalized difference values were nonzero values that maintained a relatively constant mean throughout a constant power-level region, but shifted slightly through the test profile due to power-level changes. The deviations about the mean values during constant power regions were due primarily to noise and controller responses, while the nonzero mean values are a result of engine-to-engine build variations.

The primary reason for the mean shifts at the various power levels is that the operating conditions were not consistent. For example, the calibration curve for the fuel flowmeter is nonlinear and the controller is currently capable of handling only linear functions. This results in the fuel flowmeter being optimized for a particular operating power level of the engine. Therefore while the engine controller is attempting to maintain the engine at a constant mixture ratio, it is in fact controlling the engine at different mixture ratio points due to power changes. More sophisticated regression models, that include other variables such as mixture ratio, would further reduce these shifts in the error terms.

For the Accumulative Difference Detection (ADD) algorithm, the normalized difference values for the entire set of parameters were linearly summed together, in order to produce an overall engine error value,

$$E(t) = \sum_{i=1}^{n} a_i D(t)_i \tag{2}$$

where $E(t)$ is the engine error value, n is the number of parameters in the set and $D(t)_i$ is computed by equation 1. The linear coefficients, a_i, were set at one, but can be varied to optimize the algorithm's

performance by emphasizing key parameters. For the combination of sensor data utilized, the nominal range of the engine error value was between 0.6 and -0.6.

For nominal engine tests, the overall engine error values contained significant fluctuations. A five-point average scheme was incorporated in the ADD algorithm to reduce this variation. This scheme collected five consecutive engine error values and averaged them into a single engine error value. This allowed a refinement of the tolerances and an improvement in the detection capabilities.

Zero Template Algorithm

For the second approach, the set of normalized difference values were compared to a nominal set by using the correlation technique. This technique discussed in references 7 and 8, measures the strength of the relationship between the data sets. The normalized difference values found in equation (1) for each sensor was arranged in a specific order for each data set. Each ordered set of data values is called a pattern. These patterns were developed every 40 milliseconds and were compared to a nominal standard pattern. The degree of correlation between the two patterns was determined by the correlation coefficient. This term was determined by

$$R(t)_{ij} = \frac{\mathrm{Cov}[P(t)_i, P(t)_j]}{\mathrm{SD}[P(t)_i]\,\mathrm{SD}[P(t)_j]}, \tag{3}$$

where $R(t)_{ij}$ is the correlation coefficient between the pattern at time t_i, $P(t)_i$ and the pattern at time t_j, $P(t)_j$. The functions, Cov and SD, are defined as the covariance and the standard deviation functions of the patterns, respectively. The values of the correlation coefficient range from 1 to 0, with 1 representing a perfect matching of the two patterns and values less than 1 representing the degree of deviation between the two patterns.

For the ideal case, when the regression models exactly predict the actual engine data $(D(t)_i = 0)$, normalized difference patterns should be correlated with a zero or null standard pattern. The difficulty is that correlation with any horizontal straight-line pattern results in a zero standard deviation for that pattern, and hence creates an undefined correlation coefficient.

An attempted solution to this problem was to develop a near-zero pattern or template for correlation. The nominal templates were established by averaging templates from constant power-level regions of a nominal test firing. Figure 1 shows the nominal template for the 100% rated power level (RPL) taken from test firing 902-463. Due to the ability of the PBM to closely model nominal engine operation, the normalized difference values have an order of magnitude of -2. The difficulty with this approach was that the algorithm was too sensitive to small nominal deviations in the normalized difference values due to noise, engine build, etc.

Another solution undertaken combined a zero template with an additional parameter offset. The additional parameter selected was the controller reference MCC pressure. This parameter is constant throughout stationary engine operation, never experiences failure and is available in every controller data set. A regression model was developed to predict an offset value for this parameter as a function of engine power level. Figure 2 shows the distribution of the normalized difference value for the nominal template at 100% RPL. When added to the pattern, this new error term allowed the zero template to be correlated, while at the same time it did not contribute to the correlation process. The magnitude of the offset term strongly influenced the sensitivity of the algorithm to pattern changes. Large magnitudes, greater than 0.5, made the normalized difference values, evaluated in equation (1), insignificant and skewed the correlation coefficients to 1. Small magnitudes, less than 0.1, placed the algorithm into the same situation as the near-zero pattern approach. A magnitude of approximately 0.3 was selected. This allowed the algorithm to be insensitive to nominal deviations and yet capable of detecting the failure information. Figure 3 shows the consistent behavior of the correlation coefficient when this approach was applied to nominal test firing 902-457.

This modification allowed this technique to become a feasible detection algorithm. The Zero Template Offset (ZTO) algorithm can be applied only during the constant power-level region of the

engine's operation profile. This algorithm quantified the relationship between the standard and actual normalized error value patterns into an overall engine condition value defined as the correlation coefficient.

Failure Detection Limit Development

The test data available for this investigation was from both phase I and phase II configurations of the SSME. The phase II engine provided performance improvements to the phase I engine design. The available nominal test data came from phase II test firings, while the available test failures were earlier in the testing program from the phase I engine design.

In order to develop detection limits for the two different phase engines, relative rather than absolute limits were established. During the first two seconds of steady state operation, each algorithm calculates a two second average of it's respective engine values for that particular test firing. This two second average is then established as a baseline about which the detection limits can be placed.

The detection limits were found by first evaluating ADD's and ZTO's overall engine value ranges for five nominal test cases and selecting the maximum range for each algorithm for each sensor set. These maximum ranges were then placed about the baseline value for each subsequent test firing. These limits were then tested upon the remaining nominal test cases to ensure no false-alarms from the algorithms. Once the detection limits were confirmed, the algorithms were applied to the failed test cases in order to establish detection times. The detection criteria for the ADD and ZTO algorithms were based upon one and five consecutive values, respectively, exceeding the established limits.

The development of relative detection limits made the ADD and ZTO algorithms insensitive to engine failures that manifest themselves only during the startup period. In order to compensate for some of the lost sensitivity, overall limits of ± 1 for the ADD algorithm and 0.5 for the ZTO algorithm were established. This enabled the algorithms to detect gross indications of engine failure that are initiated during startup, but do not propagate through the remainder of the test profile.

Results and Discussion

The detection capabilities for each algorithm were evaluated by applying the algorithms to twelve SSME test firings that resulted in major engine damage. The number of available sensors for each test firing varied due to sensor failures and measurements not taken. The validation of sensor data prior to analysis is important for both algorithms. This ensures that the detections made by the algorithms are based upon reliable data. A listing of the unavailable sensors for the failed SSME test firings is presented in Table 2. Some tests, such as 901-173, had 25% to 50% of the applied sensors unavailable for the algorithms to utilize.

The detection times of the ADD and ZTO algorithms are presented in Table 3, along with the detection limits used and the actual SSME redline cutoff times for each test firing. In some cases the number of unavailable sensors made the sensor set so small that multi-sensor schemes were unapplicable. This condition occurred exclusively with the LOX-side sensor set which had only six performance sensors. For either algorithm to be applied to a particular sensor set, at least three sensors had to be available, excluding the controller reference MCC pressure. For test firings where the algorithms were not applied the detection time is designated in Table 3 by 'xxx'. An omission of detection time from Table 3, indicates that the algorithms did not detect the anomaly before the current SSME redline system.

The ADD and ZTO algorithms were able to provide improved detection capability for 8 of the 12 failure test cases. These algorithms demonstrated the ability of detecting the failures, not only by their major impact to the system, but by the subtle degradations that the onset of failure can cause. The four failures not detected by these algorithms, 750-168, 902-198, 901-225 and 750-259, contained failure modes that provided no precursory information or occurred within two to three seconds after engine startup. Post-test summaries of the remaining eight detected anomalous test cases, 901-284, 901-173, 901-331, 902-249, 901-307, 901-340, 901-364 and 901-436 were extracted from references 1 and 4.

According to the post-test reports for test firing 901-284, the MCC pressure transducer become dislodged and began sensing the coolant liner pressure at t=3.9 seconds. The controller attempted to maintain the chamber pressure based upon the coolant pressure, which caused severe anomalous operation. The failure was a direct result of a failed controlled sensor and was detected by the ADD algorithm as shown in Figure 4, but not by the ZTO algorithm. The ADD algorithm detected this failure mode due to the engine error value exceeding the overall limit at 8.14 seconds after engine start. This failure mode is a controller-type failure where the engine was responding correctly to the contoller, but controller was issuing commands to the engine based upon faulty input sensor information. The magnitude of the anomalous engine performance was detectable, but no failure indication was available from the analysis of the sensor interrelationships. This result was expected, because although the engine was operating off-nominal, the engine, itself, was responding properly with the controller.

During test firings 901-173 and 901-331, the SSME experienced fracturing of the LOX posts in the main injector. Controller shutdown was initiated by high pressure turbine discharge temperature redlines at 201.16 seconds for test 901-173 and 233.14 seconds for test 901-331. Once failure occurred, the controller attempted to increase the oxidizer flow in order to maintain the engine's power level. This condition required several performance parameters to operate at points outside of their normal position, in relation to the other parameters. From the ADD application shown in Figures 5 and 6 for the fuel-side sensor set, both cases exhibited degrading engine error values during constant power-level operation. This was also reflected in pattern variations calculated from ZTO, Figures 7 and 8, for the fuel-side and total sensor sets respectively. The detection times made by both of these algorithms were done even though test 901-173 had 10 unavailable sensors, and for both tests, the high pressure fuel turbine (HPFT) discharge temperatures were unavailable. The ADD algorithm provided only slight improvements to the detection times of 184.12 seconds for test 901-173 and 232.80 seconds for 901-331. The ZTO algorithm provided failure detection times of 75.0 seconds for test 901-173 using either the fuel-side or total sensor set, while for test firing 901-331, ZTO's earliest failure detection time was at 64.56 seconds for the total sensor set.

For test 902-249, HPFT blade failure caused premature test shutdown due to accelerometer redline. According to the post-test analysis, the initial turbine damage occurred at 3.0 seconds after start of the test. At 108.0 seconds, cavitation began in the high pressure fuel pump (HPFP) due to inlet fuel temperature increases from a propellant transfer process. Through the remainder of the test the cavitation conditions worsened as the pump speed was increased to maintain fuel output. The ZTO algorithm results, Figure 9, provided an earlier detection time than the ADD algorithm results, figure 10. The ZTO algorithm detected the effect that the initial turbine damage had upon the relative parameter patterns at different power levels at 20.92 seconds. The ADD algorithm results show severe degradation of the engine error parameter due to the cavition condition and the detection limit was exceeded 158.8 seconds.

The test objective for test 901-307 was to determine the minimum upstream pressure that the LPOP could operate effectively. During 100% RPL, approximately 6 to 10 seconds into the test, the fuel preburner injector experienced a crack in a LOX injector post due to high cycle fatigue. This test continued to completion although extensive damage was caused by this failure mode. Both the ADD and ZTO algorithms were applied to the total sensor set as shown in Figures 11 and 12, and detected the engine failure mode after a scheduled power-level transition at approximately 16 seconds. These detections are based upon the relation between the engine's performances at different power levels. The test firing continued until the scheduled cutoff at 75.0 seconds.

Test 901-340 failure was a result of a progressive series of fractures that occurred in the high pressure fuel turbopump (HPFTP) turnaround duct. Figures 13 and 14 show the degradation of engine performance analyzed by ADD and ZTO algorithms respectively for the fuel-side sensor set. From the post-test report, major fractures in the turnaround duct began to occur between 277 and 290 seconds. Both algorithms indicated engine failure near this time frame, while the actual engine cutoff time, initiated by a HPFT discharge temperature redline, occurred at 405.50 seconds.

For test 901-364, a new HPFTP thermal shield retainer nut assembly allowed high temperature gases to impinge directly upon the turbine end cap. The hot gases heated up the turbine coolant, which heated up the bearings causing increased bearing stiffness and synchronous vibration. The cutoff was initiated by the preburner boost pump radial accelerometer at 392.15 seconds after start of the test. Figures 15 and 16 show the engine's response to the failure mode as evaluated by the ADD and ZTO algorithms applied to the fuel-side sensor set. Thoughout the constant power-level regions of the test profile, these engine error values continue to degrade and detection of the failure mode was made at 45.24 seconds for the ADD and 38.0 seconds for the ZTO, well in advance of the controller system.

For test 901-436, shutdown was initiated by the HPFT discharge temperature redline due to buckling of the HPFTP coolant liner. According to post-test reports, the HPFTP had an abnormally high vibrational amplitude from 10 to 213 seconds, then this amplitude began to decline along with the HPFP efficiency. The response by the HPFTP coolant pressure and temperature to the failure mode began at 598.5 seconds and cutoff was initiated at 611.06 seconds due to a HPFT discharge temperature redline. The engine error values calculated by ADD and ZTO algorithms for the total sensor set are shown in Figures 17 and 18. Both of these values responded to the continuous HPFTP degradation mode and both algorithms detected failure indications well in advance of the responses exhibited within the HPFTP coolant liner. The ZTO algorithm detected the failure during the abnormally high vibration period at 141.04 seconds. During the decline of the fuel pump efficiency, the ADD algorithm detected the failure at 325.92 seconds.

For both algorithms, the fuel-side parameter set provided detection more often than the LOX-side parameter set. This was due to the removal of several key parameters from this set, such as the HPOT discharge temperature, that had to be discarded because of their response to venting conditions. Improvements to the regression models, that would compensate for the venting condition responses would allow inclusion of these parameters and thereby extend the detection capabilities of the LOX-side parameter set.

As shown in Table 3, for the ADD algorithm the ability of the total sensor set to map the performance of the entire system appeared to be as effective as the fuel-side parameter set. While the addition of the LOX-side parameters delayed the detection time for some test firings, it improved detection times for others. For the ZTO algorithm, the combined parameter set provided detection times equivalent to, or better than, those obtained by the fuel-side parameter set. The additional LOX parameters improved the pattern analysis capability by providing a more complete response pattern of the engine.

In order to test the robustness of these algorithms to sensor failures, several parameters were removed from anomalous test firings to simulate sensor failure and the changes in their detection times were observed. Six test cases were conducted upon the total sensor set for three anomalous test firings, 901-340, 901-364 and 901-436, and one nominal test firing. The first test case involved the initial total sensor set that each test firing had available with no additional sensor elimination and resulted in detection times identical to those shown in Table 3. Each subsequent test case included an additional sensor eliminated from the total sensor set. The eliminated sensor, in the order of elimination, are by PID; 59, 18, 261, 17 and 52. Figure 19 shows the changes in the ADD and ZTO detection times for each test case and each test firing. For the nominal test firing, no false alarms were indicated for any of the test cases applied. In general, the effect of eliminating sensors degraded the detection performance, but several cases showed an improvement in the detection performance of the algorithms. Therefore the number of parameters that are effected by the current failure mode and are available to the algorithms, dictate the algorithms' ability to detect that failure. Also in some cases, the affects of the failure mode can be masked by other unaffected normalized-difference values in the sensor set.

Concluding Remarks

Two algorithms were developed that combined information from several SSME performance parameters into single detectable engine values. These values were then monitored to detect engine failure.

For eight of the twelve anomalous test firings available, these algorithms demonstrated earlier detection times than the current SSME safety monitoring system. Of the eight detected anomalous test firing, the ADD algorithm detected all eight, while the ZTO algorithm detected seven of the eight. No false alarms were indicated by either algorithm for twelve nominal test firings and both algorithms are robust to sensor failure. Both of the proposed multi-sensor algorithms demonstrated the safety monitoring features necessary to complement the current SSME safety monitoring system.

Irrespective of the sensor set, the ZTO algorithm provided significantly earlier detection times than the ADD algorithm for several of the detected anomalous test firings. This was because the ZTO offered a more complex analysis by quantifying the interrelationships of the parameter responses, where the ADD analyzed only the magnitude between the actual and predicted values. One advantage ADD has over the ZTO algorithm is the capability to detect a controller-type failure mode that occurs during or before startup, such as test firing 901-284. For this type of failure mode, the controller was issuing commands based upon erroneous sensor data. If this failure were to occur during the mainstage of the test, an overall limit applied to ZTO would have allowed detection of the failure.

Additional training of these algorithms is recommended to ensure that the detection limits do not initiate false alarms and yet provide the engine with the optimum detection capabilities. These training sets should also include data from both nominal and anomalous SSME test firings. Enhancement of the regression models by including affects from venting operations, would provide a more accurate perdiction of the performance parameters and allow the two LOX-side parameters previously excluded to be analyzed. Additional studies are recommended to optimize the linear coefficients in the ADD algorithm and the magnitude of the offset term for the ZTO algorithm.

Acknowledgment

This work was supported by the NASA Lewis Research Center under contract NAS3-25266 with Larry P. Cooper as monitor.

References

1. Taniguchi, M. H., *Failure Control Techniques for the SSME, Phase I Final Report*, NASA CR-179224, 1986.

2. Cikanek, H. A., *Characteristics of Space Shuttle Main Engine Failures*, AIAA Paper 87-1939, AIAA/SAE/ASME/ASEE 23rd Joint Propulsion Conference, June 29-July 2, 1987.

3. Cikanek, H. A., *SSME Failure Detection*, 4th American Control Conference Proceedings, Vol. 1, New York, Institute of Electrical and Electronic Engineers, 1985, pp 282-286.

4. Hawman, M. H.; Galanitis, W. S.; Tulpule, S.; Mattedi, A., *Framework for a Space Shuttle Main Engine Health Monitoring System, Final Report*, NASA CR - 185224, May 1990.

5. Taniguchi, M. H., *Failure Control Techniques for the SSME, Phase II Final Report*, NASA CR-179231, 1987.

6. Nemeth, E., *Health Management System for Rocket Engines, Final Report*, NASA CR-185223, June 1990.

7. Ehrenberg, A. S. C., Data Reduction, Analysing and Interpreting Statistical Data, John Wiley & Sons, London, 1975, pp. 233-238.

8. Young, H. D., Statistical Treatment of Experimental Data, McGraw-Hill Book Company, New York, 1962, pp. 126-132.

Table 1. Breakdown of the total sensor set into fuel-side and oxidizer-side subsets.

Fuel-Side Parameter Subset

287	Controller Reference MCC Pressure
32	LPFP Shaft Speed
225	LPFP Discharge Temperature Channel A
226	LPFP Discharge Temperature Channel B
52	HPFP Discharge Pressure
58	Fuel Preburner Chamber Pressure
260	HPFP Shaft Speed Channel A
261	HPFP Shaft Speed Channel B
231	HPFT Discharge Temperature Channel A
232	HPFT Discharge Temperature Channel B
24	MCC Hot Gas Injector Pressure
17	MCC Coolant Discharge Pressure
18	MCC Coolant Discharge Temperature
59	PBP Discharge Pressure

Oxidizer-Side Sensor Subset

287	Controller Reference MCC Pressure
59	PBP Discharge Pressure
93	PBP Discharge Temperature Channel A
94	PBP Discharge Temperature Channel B
90	HPOP Discharge Pressure
30	LPOP Shaft Speed
21	MCC Oxidizer Injector Temperature

Table 2. Unavailable sensors for each SSME failed test firing listed by PID number.

Anomalous Test Firing Number	Unavailable Sensors
750-168	58,21
901-173	52,58,231,232,18,93,94,90,30,21
902-198	21
901-225	231,232,93,94,21
902-249	58
750-259	52,30,21
901-284	226,261,232,18,59
901-307	
901-331	58,231,232,59
901-340	58,231,232,94,90,30,21
901-364	21
901-436	

Table 3. Results of the application of ADD and ZTO algorithms to the available SSME test Failures.

Anomalous Test Firing Number	ADD Detection Time (sec.)			ZTO Detection Time (sec.)			SSME Redline Cutoff Time (sec.)
	Fuel Side Set Limit=0.13	LOX Side Set Limit=0.095	Total Set Limit=0.148	Fuel Side Set Limit=0.05	LOX Side Set Limit=0.025	Total Set Limit=0.05	
750-168							300.20
901-173	184.12	xxx	194.12	75.00	xxx	75.00	201.16
902-198							8.50
901-225							255.61
902-249	158.80		159.40	20.92	88.6	20.92	450.58
750-259							101.50
901-284	8.14	8.14	8.14				9.88
901-307	15.84	15.84	15.64	15.64		15.64	75.00
901-331	232.80		232.80	232.56		64.56	233.14
901-340	279.24	xxx	279.24	290.24	xxx	290.24	405.50
901-364	45.24		107.92	38.00		38.04	392.15
901-436	448.32		325.92	177.44		141.04	611.06

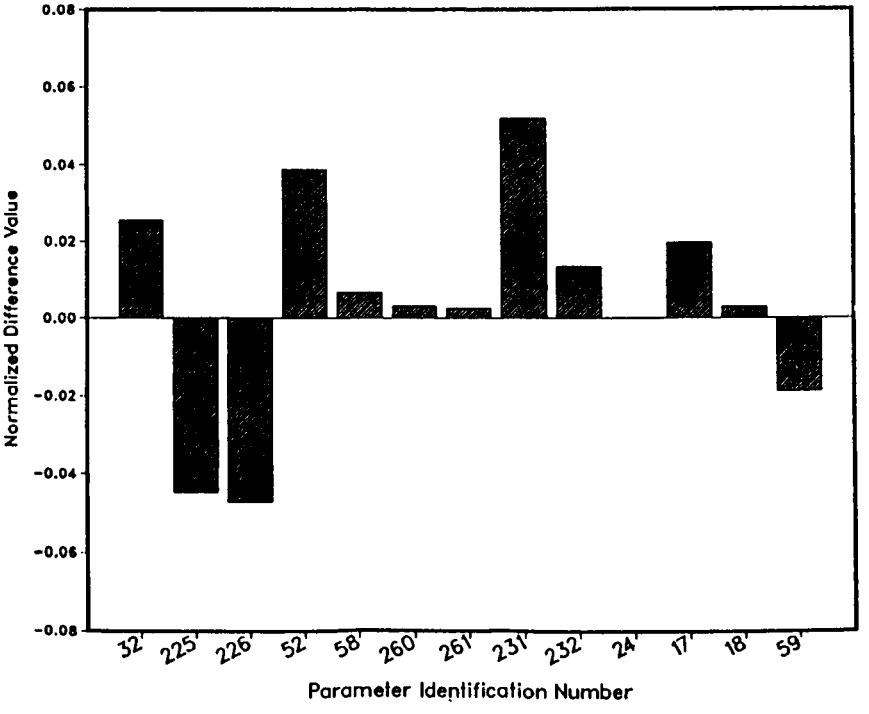

Figure 1. The nominal template utilized at the 100% rated power level in the near-zero template solution attempt.

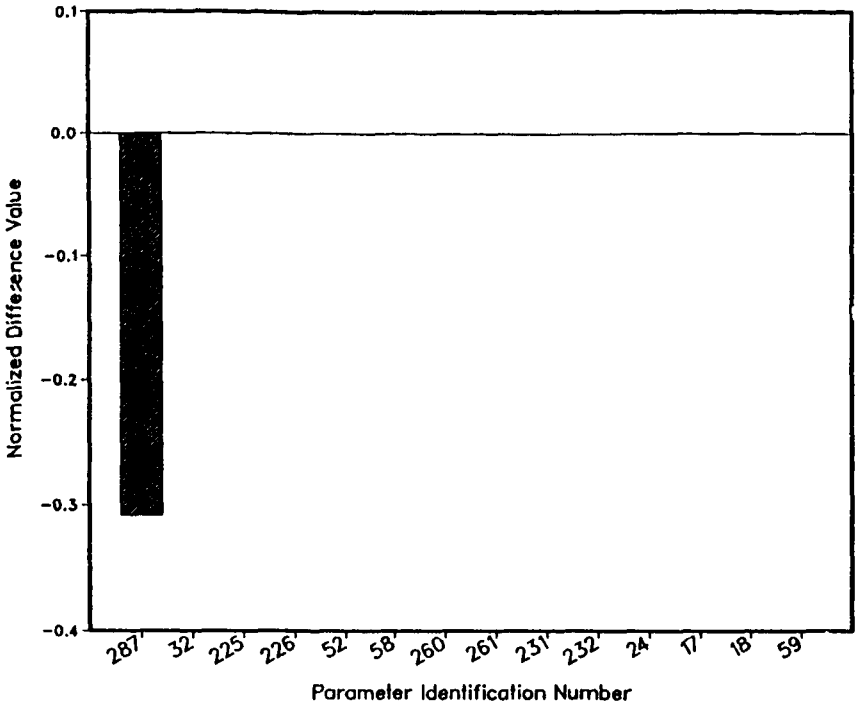

Figure 2. The nominal template utilized at the 100% rated power level in the zero template plus offset attempt.

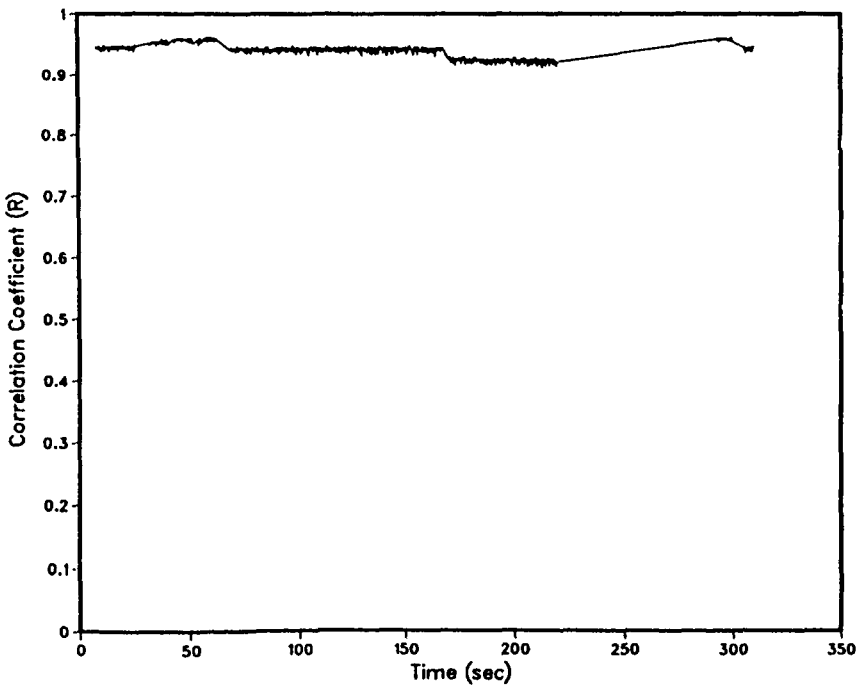

Figure 3. The zero template plus the offset term correlated to the templates from nominal test firing 902-457.

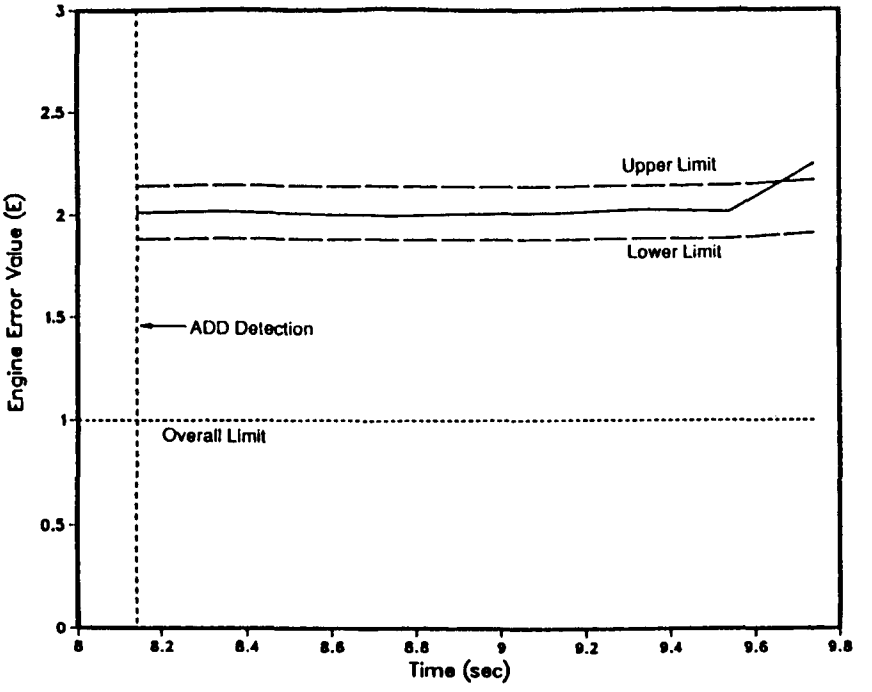

Figure 4. The ADD algorithm applied to the fuel-side sensor set for test 901-284.

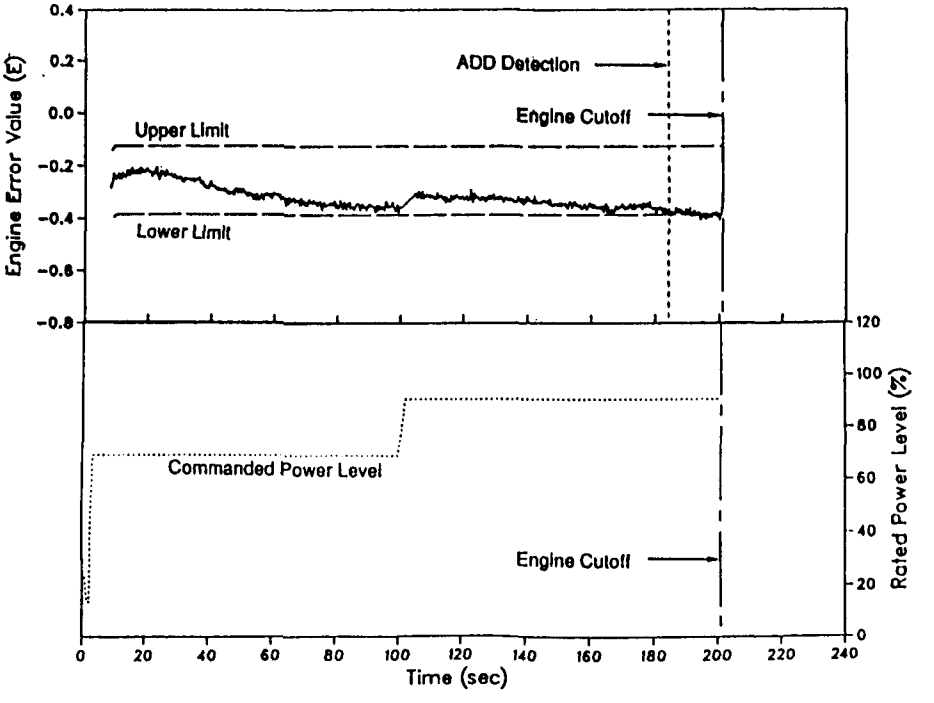

Figure 5. The ADD algorithm applied to the fuel-side sensor set for test 901-173.

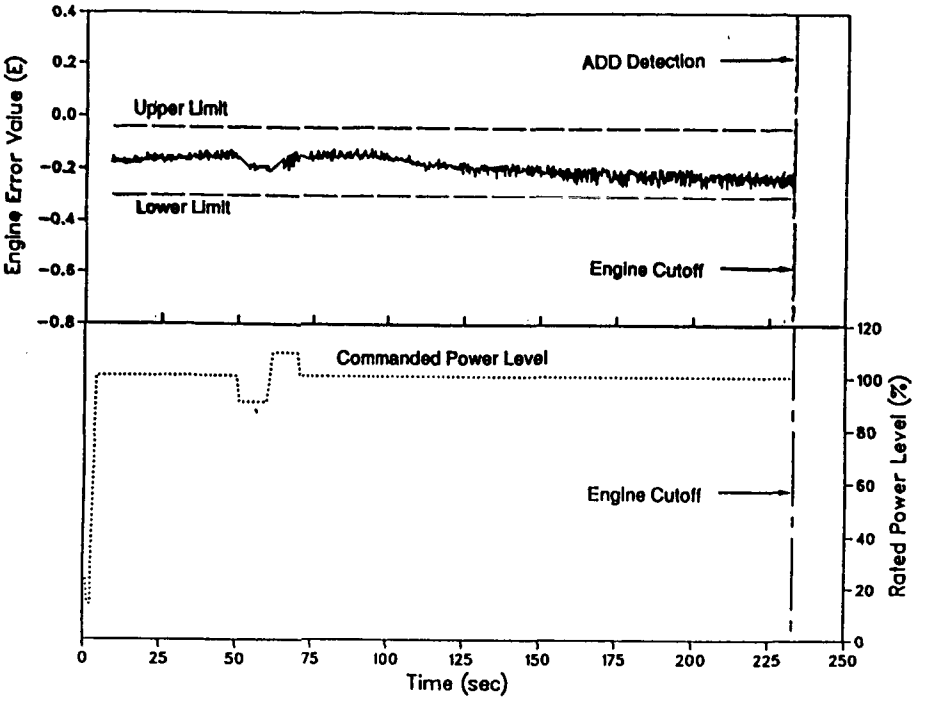

Figure 6. The ADD algorithm applied to the fuel-side sensor set for test 901-331.

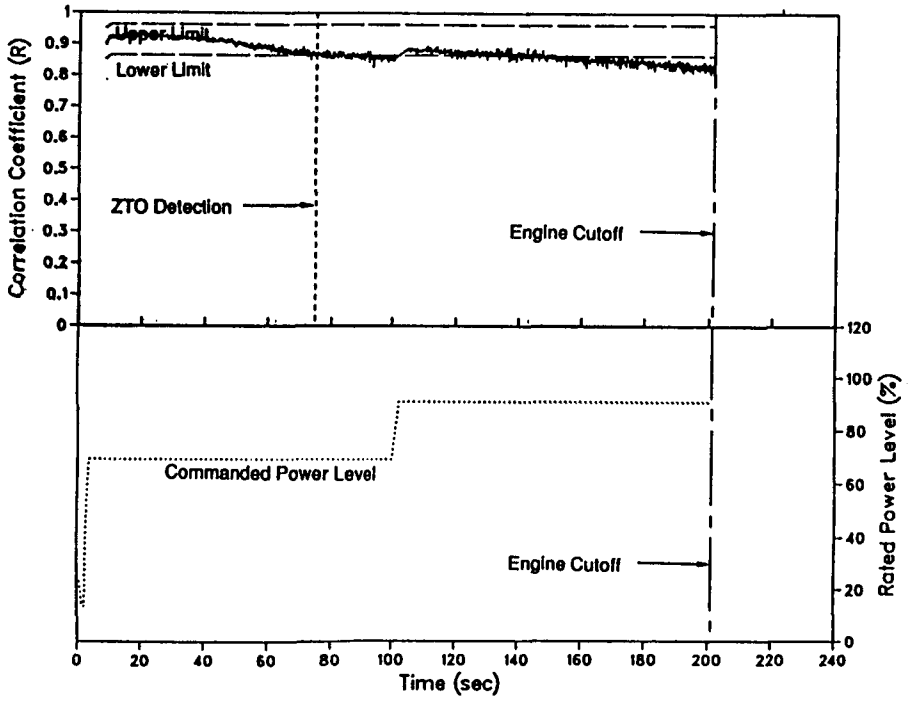

Figure 7. The ZTO algorithm applied to the fuel-side sensor set for test 901-173.

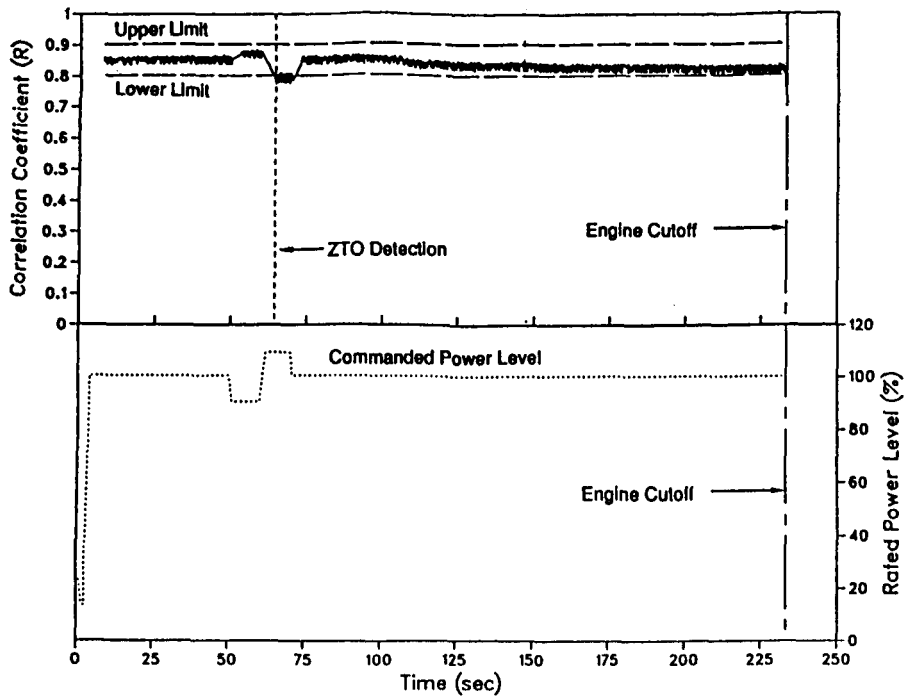

Figure 8. The ZTO algorithm applied to the total sensor set for test 901-331.

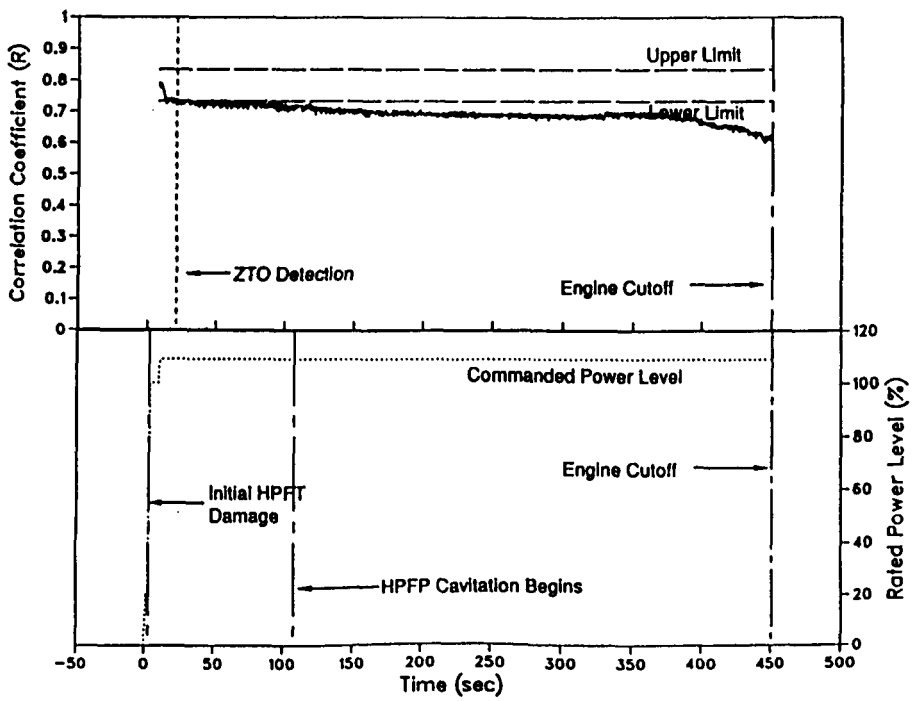

Figure 9. The ZTO algorithm applied to the fuel-side sensor set for test 902-249.

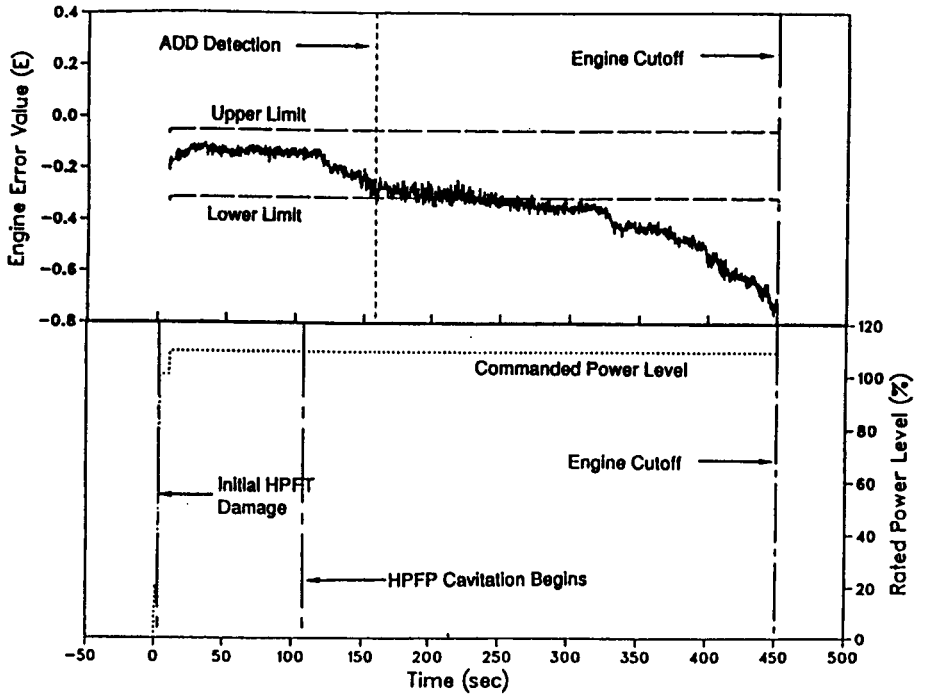

Figure 10. The ADD algorithm applied to the fuel-side sensor set for test 902-249.

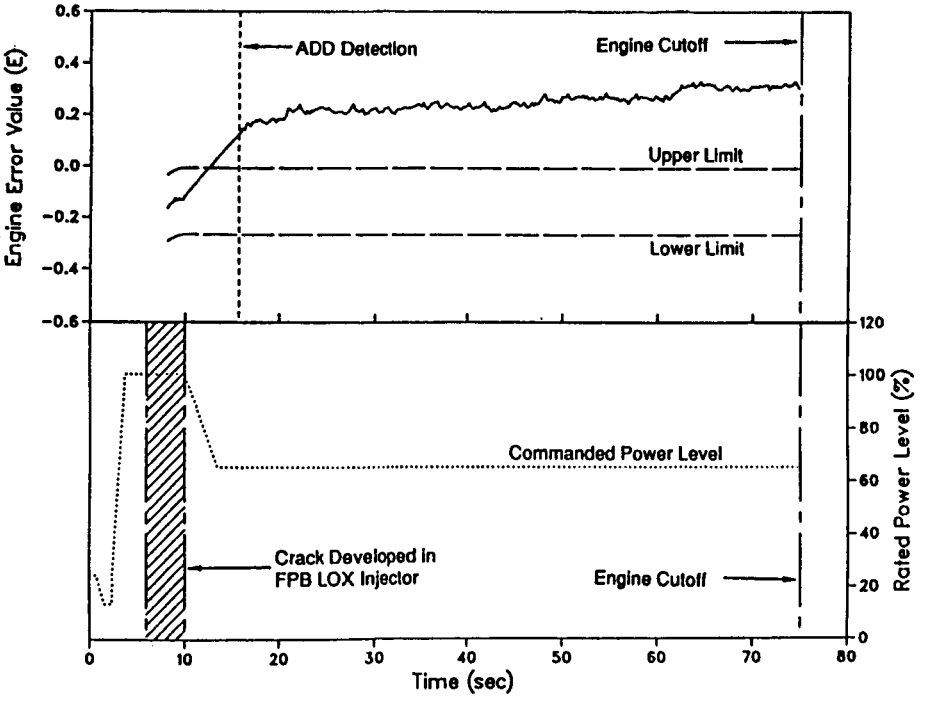

Figure 11. The ADD algorithm applied to the total sensor set for test 901-307.

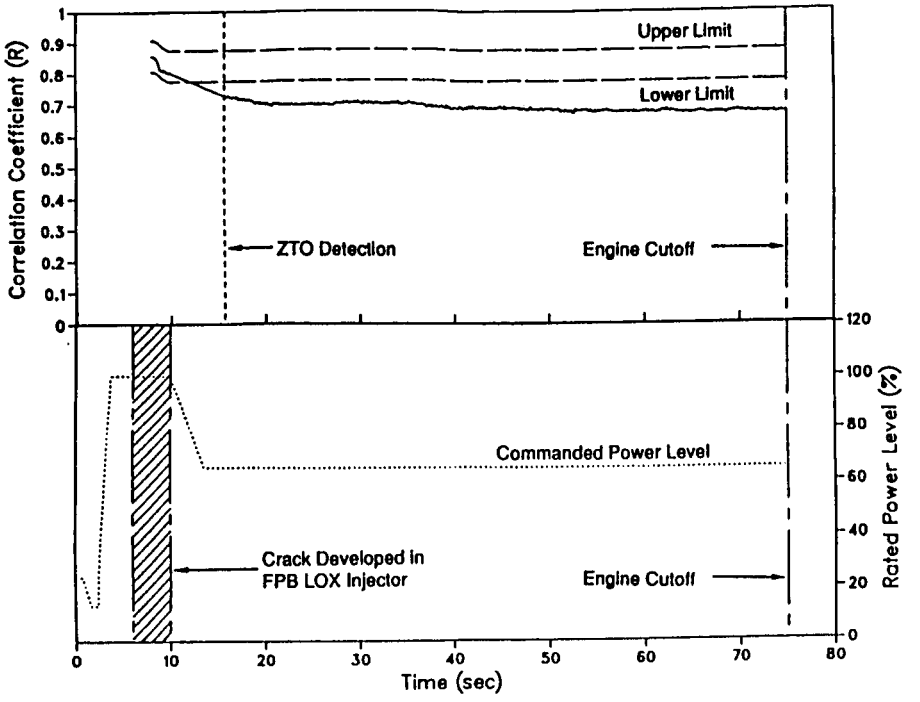

Figure 12. The ZTO algorithm applied to the total sensor set for test 901-307.

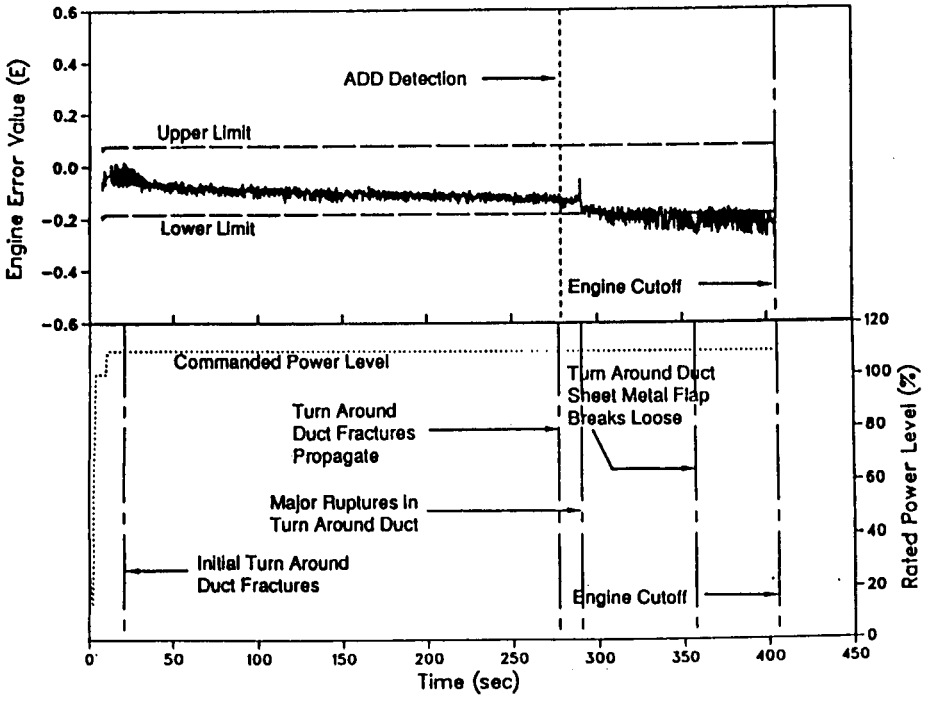

Figure 13. The ADD algorithm applied to the fuel-side sensor set for test 901-340.

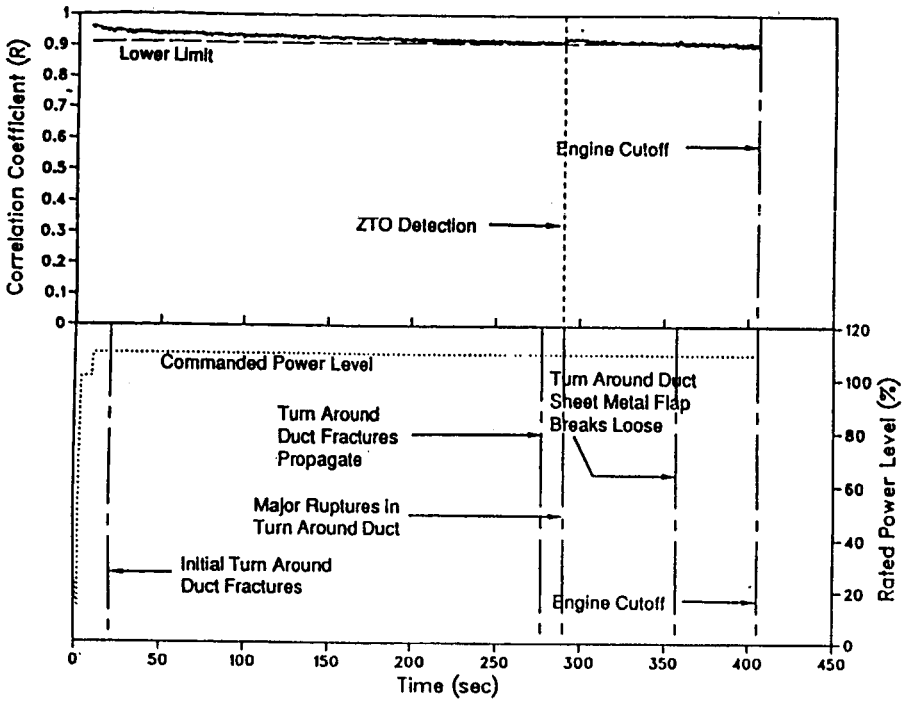

Figure 14. The ZTO algorithm applied to the fuel-side sensor set for test 901-340.

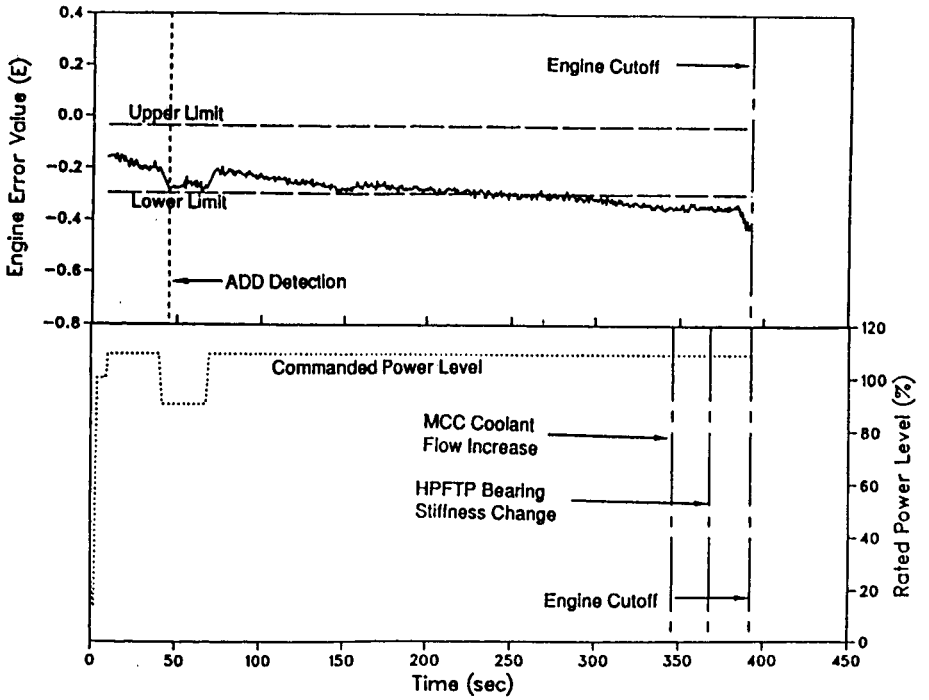

Figure 15. The ADD algorithm applied to the fuel-side sensor set for test 901-364.

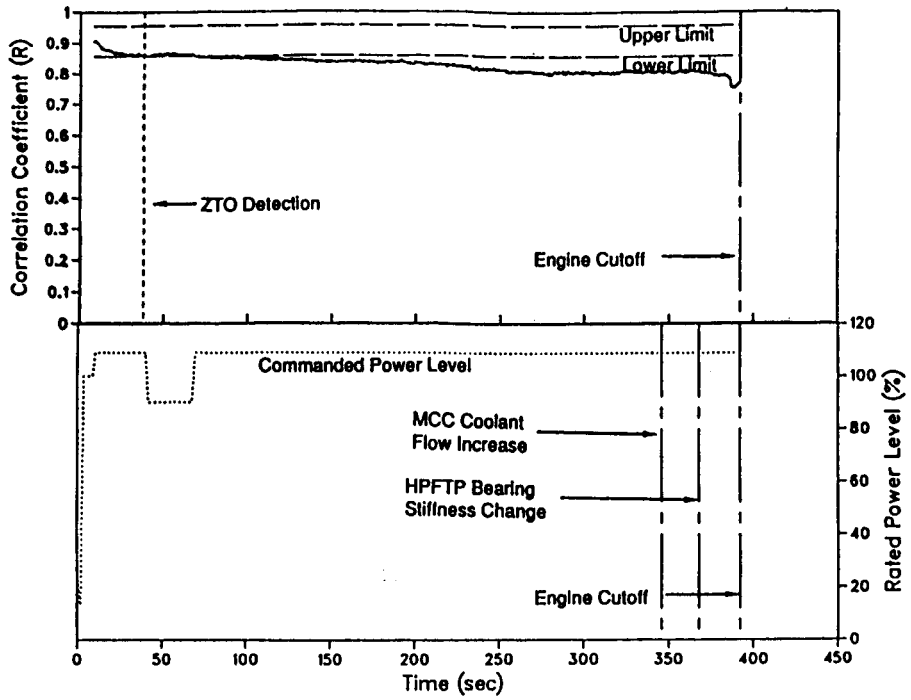

Figure 16. The ZTO algorithm applied to the fuel-side sensor set for test 901-364.

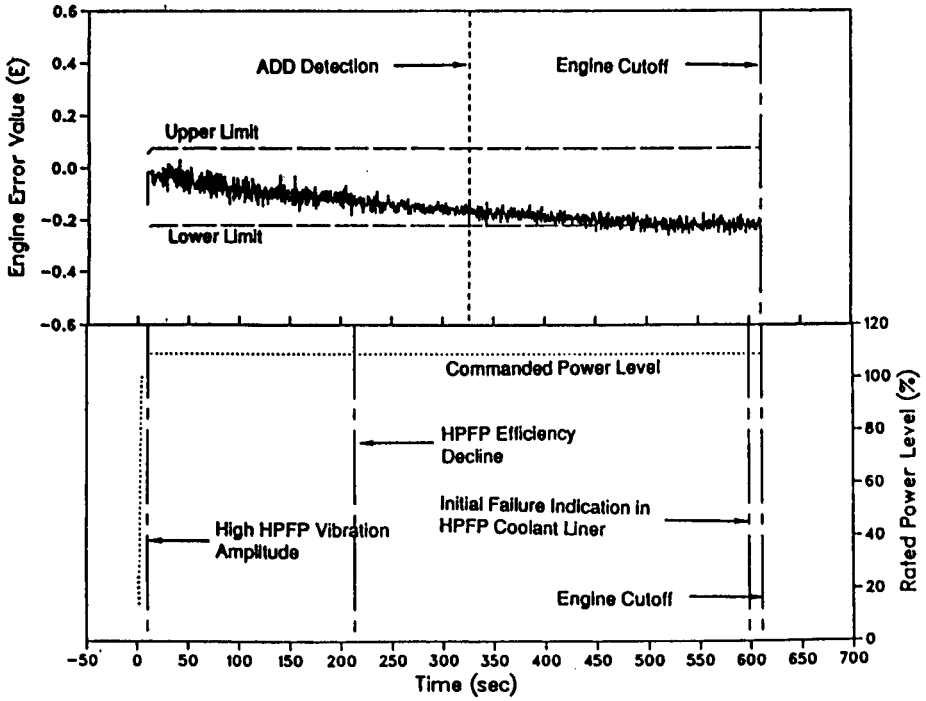

Figure 17. The ADD algorithm applied to the total sensor set for test 901-436.

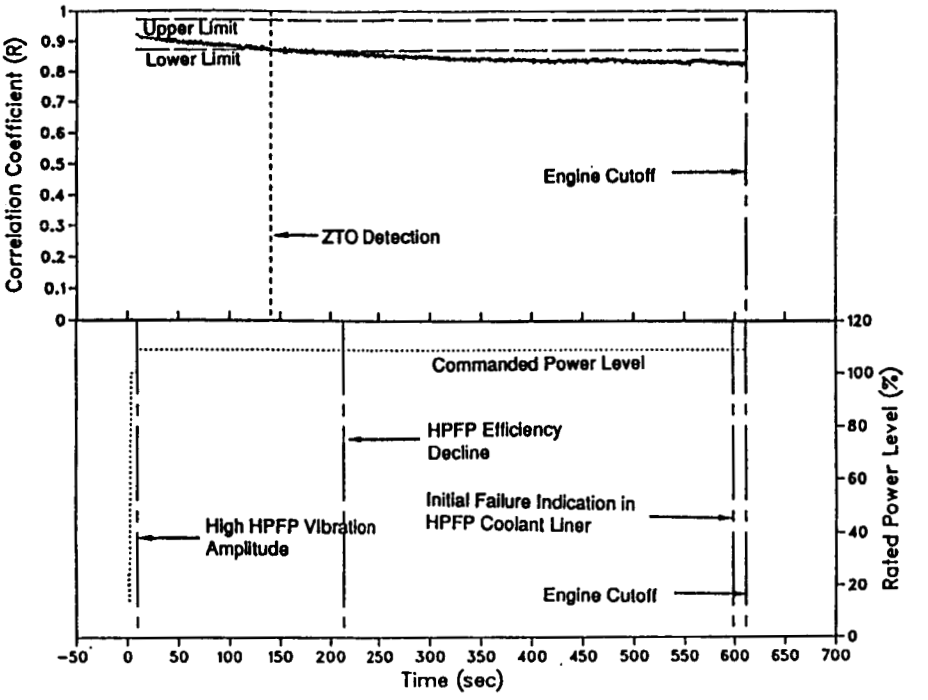

Figure 18. The ZTO algorithm applied to the total sensor set for test 901-436.

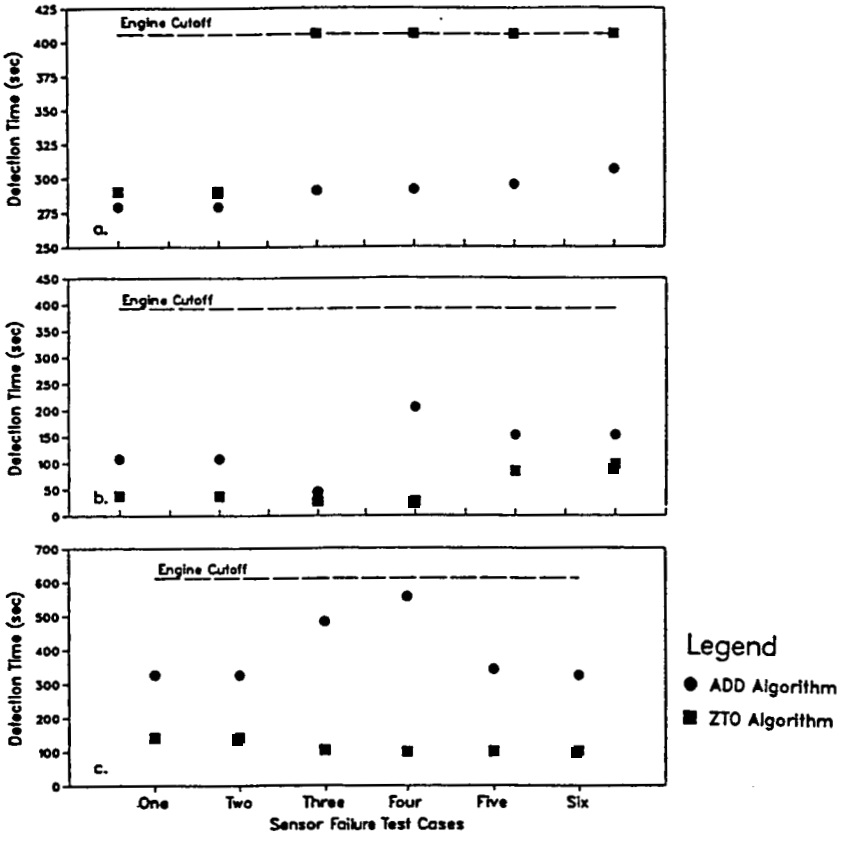

Figure 19. The ADD and ZTO detection times for the sensor failure test cases applied to (a) 901-340, (b) 901-364 and (c) 901-436 for the total sensor set.

NASA
National Aeronautics and Space Administration

Report Documentation Page

1. Report No.	2. Government Accession No.	3. Recipient's Catalog No.
NASA CR-185260 AIAA-90-1990		

4. Title and Subtitle

Multi-sensor Analysis Techniques for SSME Safety Monitoring

5. Report Date

6. Performing Organization Code

7. Author(s)

William A. Maul III

8. Performing Organization Report No.

None (E-5591)

10. Work Unit No.

553-13-00

9. Performing Organization Name and Address

Sverdrup Technology, Inc.
Lewis Research Center Group
2001 Aerospace Parkway
Brook Park, Ohio 44142

11. Contract or Grant No.

NAS3-25266

13. Type of Report and Period Covered

Contractor Report
Final

12. Sponsoring Agency Name and Address

National Aeronautics and Space Administration
Lewis Research Center
Cleveland, Ohio 44135-3191

14. Sponsoring Agency Code

15. Supplementary Notes

Project Manager, Larry P. Cooper, Space Propulsion Technology Division, NASA Lewis Research Center. Prepared for the 26th Joint Propulsion Conference cosponsored by the AIAA, SAE, ASME, and ASEE, Orlando, Florida, July 16-18, 1990.

16. Abstract

Two algorithms were developed which utilized multi-sensor analysis techniques to complement the current Space Shuttle Main Engine (SSME) safety monitoring system. The first algorithm analyzed the accumulative error between actual and predicted values of the engine parameter set, while the second algorithm combined these error terms into a response pattern and correlated each pattern with a standard pattern. These algorithms were applied to twelve SSME anomalous test firings and were found to produce improved failure detection times in eight of those twelve compared to the current engine safety monitoring system. Of the eight detected anomalous test firings, the first algorithm detected all eight, while the second algorithm detected seven of the eight. No false alarms were indicated by either algorithm for twelve nominal test firings. An initial parametric study of these algorithms for optimized parameter selection is presented and algorithm robustness to sensor failure is demonstrated.

17. Key Words (Suggested by Author(s))	18. Distribution Statement
Space Shuttle Main Engine; Rocket engine; Safety monitoring; Pattern recognition; Multi-variable correlation	Unclassified – Unlimited Subject Category 15, 20

19. Security Classif. (of this report)	20. Security Classif. (of this page)	21. No. of pages	22. Price*
Unclassified	Unclassified	20	A03

NASA FORM 1626 OCT 86

*For sale by the National Technical Information Service, Springfield, Virginia 22161